An optimized design of SOI-based AWGs for (de)multiplexer applications

Shibnath Pathak,[1,*] Dries Van Thourhout,[1] and Wim Bogaerts[1]

[1] *Photonics Research Group (INTEC), Ghent University - imec, Sint-Pietersnieuwstraat 41, B-9000 Ghent, Belgium*

compiled: June 15, 2013

We demonstrate compact SOI based arrayed waveguide gratings (AWG) for (de)multiplexing applications with a large free spectral range (FSR). The large FSR is obtained by reducing the arm aperture pitch without changing the device footprint. We demonstrate 4×100 GHz, 8×250 GHz and 12×400 GHz AWGs with an FSR of 6.9nm, 24.8nm, 69.8nm respectively. We measured an insertion loss from -2.45dB for high to -0.53dB for low resolution AWGs. The crosstalk varies between 17.12dB to 21.37dB. The bandwidth remains nearly constant and the non-uniformity between the center wavelength channel to the outer wavelength channel improves with larger FSR values.

OCIS codes: (130.0130) Integrated optics; (130.1750) Components; (130.7408) Wavelength filtering devices; (130.3120) Integrated optics devices.

http://dx.doi.org/10.1364/XX.99.099999

1. Introduction

Arrayed Waveguide Gratings (AWGs) are a commonly used component in Wavelength Division Multiplexing (WDM) systems for wavelength (de)multiplexing [1] and routing applications [2]. AWGs are realized in different material platforms and cover various wavelength ranges. Different platforms impose different design restrictions and opportunities for both the star couplers and the array waveguides. Compared to low contrast material platforms such as silica-on-silicon and InP [3, 4], high contrast silicon-on-insulator (SOI) waveguides allow much sharper bends, reducing the device size by several orders of magnitude . But the high contrast waveguides also have a higher propagation loss and are highly sensitive to phase errors. As a result, demonstrated silicon AWGs [5–7] exhibit a relatively high insertion loss and crosstalk, especially in devices with higher resolution, which require longer and more delay lines in the waveguide array. Therefore, in SOI it is difficult to design AWG demultiplexers with small channel spacing and large free spectral range (FSR).

In this paper we propose an improved design procedure which leads to an optimized performance for such devices. We illustrate this procedure through the design and characterization of three sets of SOI AWGs with 100 GHz, 250 GHz and 400 GHz channel spacing respectively. The devices are analyzed in terms of insertion loss, crosstalk, bandwidth and non-uniformity between the center and outer channels. Clear trends towards optimized designs are observed.

* Shibnath.Pathak@intec.UGent.be

2. Theory

The constant length difference (ΔL) between two successive waveguides in the array section of an AWG sets its free spectral range (FSR):$\Delta\lambda_{\mathrm{FSR}} = \lambda_{\mathrm{c}}^2/(n_{\mathrm{group}}\Delta L)$, where n_{group} is the group index of the waveguide, λ_{c} is the center wavelength and $\Delta\lambda_{\mathrm{FSR}}$ is the FSR. The dispersion $\mathrm{D} = \Delta s/\Delta\lambda$ of the waveguide array, defined as the displacement of the focal spot along the image plane per unit of wavelength change is given by:

$$\mathrm{D} = \mathrm{R}_a \frac{\Delta\theta_a}{\Delta\lambda} \tag{1}$$

$$= \frac{\mathrm{R}_a}{\Delta\lambda}\mathrm{asin}\left[\left(\frac{\lambda_{\mathrm{c}}}{d_a\Delta\lambda_{\mathrm{FSR}}}\right)\left(\frac{\lambda_{\mathrm{c}}n_{\mathrm{eff}}(\lambda) - \lambda n_{\mathrm{eff}}(\lambda_{\mathrm{c}})}{n_{\mathrm{group}}n_{\mathrm{slab}}(\lambda_{\mathrm{c}})}\right)\right] \tag{2}$$

where $n_{\mathrm{slab}}(\lambda_{\mathrm{c}})$ is the effective index of the waveguide mode in the slab regions at the center wavelength λ_{c}, R_a is the focal length of the free propagation region (shown in Fig. 1(d)), θ_a is the diffraction angle and d_a is the arm aperture pitch. As shown in Fig. 1(d)) d_a is determined by the sum of the aperture waveguide width and the gap between two neighboring waveguides (with this gap chosen as the minimum spacing allowed by the technology platform, typically 100 nm in our case). If we keep the channel spacing and the dispersion fixed, increasing the FSR requires either increasing the focal length (R_a) or decreasing the arm aperture pitch d_a.

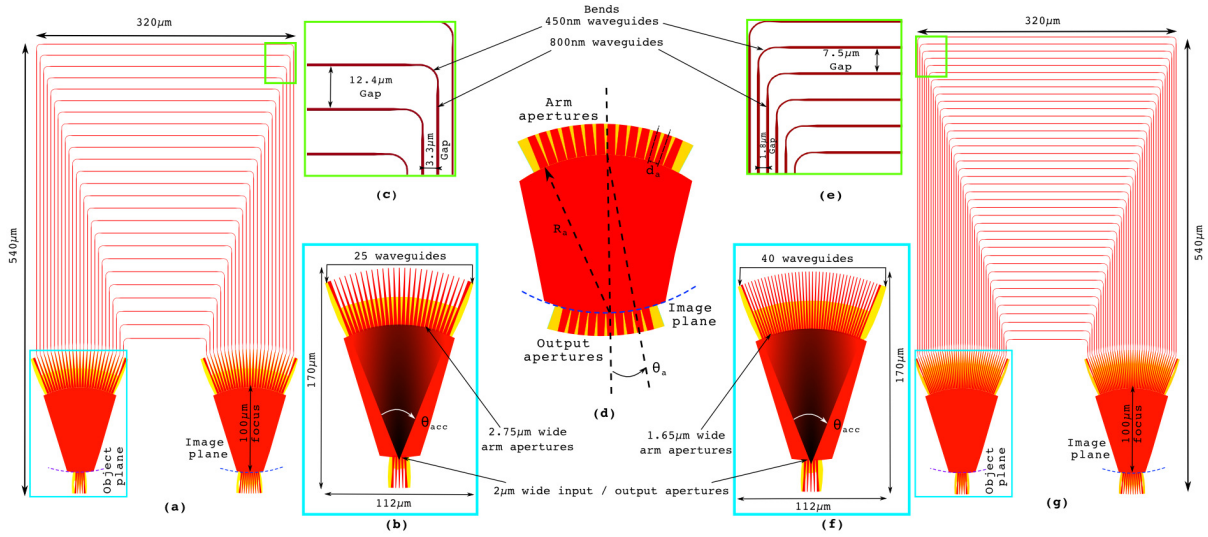

Fig. 1. Design details of 12×250 GHz AWGs. (a) The device with 25 waveguides in the array. (g) The device with 40 waveguides in the array. (b) and (f) input star-coupler of the device (a) and (g) respectively. (c) and (e) Zoom into waveguide array regions for the device (a) and (g) respectively. (d) Details overview of the star coupler.

Table 1. Design overview of three AWG sets

Sets (size)	Waveguides	Arm aperture width(μm)	Order	Delay length(μm)	FSR (nm)
4×100	16	3.49	254	146.15	4.3
GHz	20	2.75	230	116.81	5.3
(1180×285	24	2.26	169	97.25	6.4
μm^2)	28	1.91	145	83.44	7.5
8×250	25	2.75	65	37.4	16.8
GHz	30	2.26	54	31.07	20.2
(540×320	35	1.91	47	27.05	23.2
μm^2)	40	1.65	41	23.59	26.6
12×400	40	2.01	26	14.96	42.0
GHz	50	1.57	20	11.51	54.6
(380×330	60	1.28	17	9.78	64.2
μm^2)	70	1.07	15	8.63	72.8

The first option, increasing R_a, results in a significantly increased device size and associated with that a larger propagation loss, a stronger defocussing effect [8] and increased phase errors, all undesirable. On the other hand, if we increase the FSR by decreasing d_a the total device size remains the same: given that the total acceptance angle θ_{acc} of the array remains the same this option does mean we have to increase the number of waveguides ($\theta_{acc} = N \times d_a$) but as the FSR scales inversely proportional to ΔL the maximum waveguide length remains the same. As an example Fig. 1 (a) and (f) show two 8×250 GHz AWGs with arm aperture widths of 2.75μm resp. 1.65μm, and 25 resp. 40 waveguides in the array. The total footprint remains unchanged between both devices, but the FSR has increased from 16.8 nm to 26.6 nm by decreasing the aperture width.

Decreasing the arm aperture pitch has significant impact on the performance of the AWG. The propagation loss and the imaging quality of the array are the main factors contributing to the insertion loss of the device. Given that the average length of the delay lines remains unchanged, the total propagation loss will not increase.

Furthermore, for a fixed number of channels, the increasing FSR will decrease the roll-off of the transfer characteristic for the outer channels, resulting in a smaller nonunformity between the inner and outer channels. This can be explained by the fact that the spectral response of the AWG follows the envelope of the farfield of a single arm aperture. A narrower arm aperture has a wider farfield, resulting in a slower roll-off for positions near the center. The bandwidth of the individual wavelength channels on the other hand will remain constant as the channel spacing, the dispersion in the object plane (D) and the width of the input and output apertures are kept fixed with the variation of the arm aperture pitch and the FSR. This also implies that the neighboring channel crosstalk will remain unchanged for the larger FSR devices. Also the effect on the crosstalk floor due to phase error in the waveguide array will be small as the average length of the waveguide remains unaltered.

The main limitation to further increasing the number of waveguides and the FSR is the decreasing spacing between the waveguides in the array itself as shown in the Fig 1 (c) and (d). The reduced distance can introduce coupling between the waveguides, possibly resulting in additional phase errors. Another limitation is that we cannot reduce the arm aperture width below its critical width, for which the mode is no longer confined in the core of the waveguide and the propagation loss increases significantly.

3. Design

All the AWGs were fabricated on 200mm SOI wafers with a 220nm thick silicon guiding layer on top of a

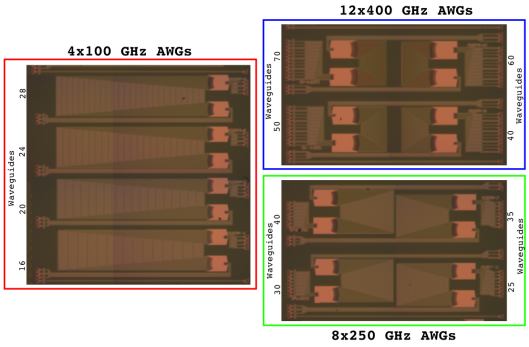

Fig. 2. Optical images of the fabricated AWGs.

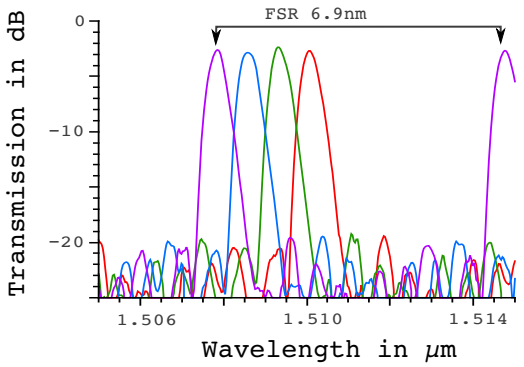

Fig. 3. Experimental spectral response of 4×100 GHz AWG with 28 waveguides used in the array.

2μm buried oxide layer. To pattern the designs we used 193nm deep UV lithography and a double etch process: 220nm deep trenches define the high contrast waveguides (further referred to as the deep etch) as well as the sharp bends and a 70nm etch defined fiber grating couplers and lower contrast apertures in the star coupler regions (further referred to as shallow etch). See [9] for further fabrication details.

We designed three sets of AWGs for three different channel spacings. Each of these three sets (4×100 GHz, 8×250 GHz and 12×400 GHz) of AWGs has four variations of the number of waveguides used in the array waveguides thereby also varying the FSR (see section 2). See [5, 6] for design details of the SOI AWGs. The focal length of the star couplers was kept constant for each of those sets of AWG designs at 80μm, 100μm and 120μm respectively. Table 1 gives further design details for each of the fabricated devices.

4. Result and Discussion

To characterize the AWGs the input and output channels are connected to 1D grating couplers (as shown in Fig. 2). The coupling efficiency [10] with standard single mode fiber is nearly 30%. In the measurements reported here we normalized the transmission spectrum of the AWGs with respect to that of a straight waveguide with the same type of grating couplers. The optical fibers were aligned to the grating couplers on an automated alignment setup, which uses a reproducible and wavelength-corrected algorithm to align with an accuracy of 0.01μm in X, Y, Z directions. Fig. 2 shows optical microscope images of the fabricated AWGs.

Figure 3, 4 and 5 show the measured spectral response of the 4×100 GHz, 8×250 GHz and 12×400 GHz AWGs using 28, 40 and 70 waveguides in the array respectively. The measured FSR for these devices was 6.9nm, 24.8nm and 69.8nm respectively. It is immediately obvious that the loss and the crosstalk improve considerably when increasing the AWG channel spacing.

4.A. Insertion loss and non-uniformity

Figure 6(a) shows how the insertion loss changes with the variation of the number of waveguides used in the waveguide array. As already mentioned above, the insertion loss improves when going from 100GHz to 200GHz and then 400GHz channel spacing, which is related to the decrease in device size and associated propagation loss. Within one device group the insertion loss improves when increasing the number of waveguides, as predicted in section 2. Further improvement is restricted by the critical width of the shallow etched arm apertures to avoid high propagation loss due to an unconfined mode. Figure 6(b) shows the non-uniformity in the insertion loss between the center channel and the outer channel as function of the number of waveguides in the array. As expected from the reasoning in the previous paragraph the uniformity improves with increasing FSR.

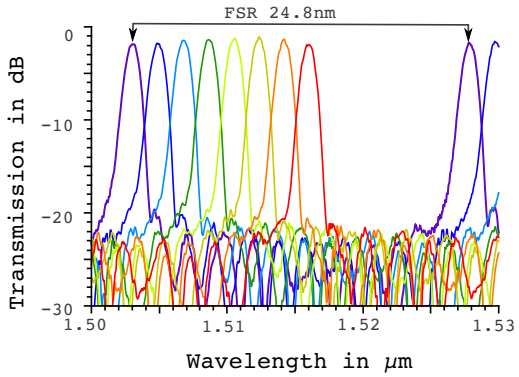

Fig. 4. Experimental spectral response of 8×250 GHz AWG with 40 waveguides used in the array.

4.B. Crosstalk

Due to the high confinement of silicon waveguides, even small geometric variations introduce significant phase errors, resulting in an unwanted crosstalk floor. Fig. 6(c) shows how the crosstalk level changes with the number of waveguides used in the array. The crosstalk level is defined by taking the difference (in dB) between the crosstalk floor and the center channel loss and as can

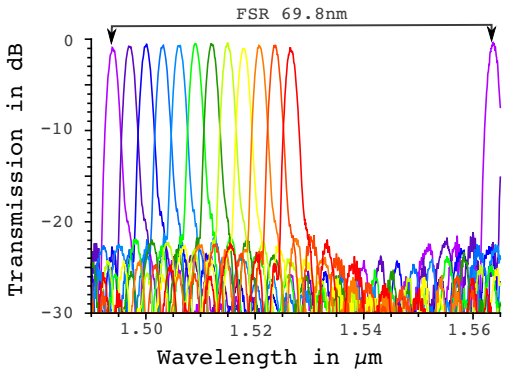

Fig. 5. Experimental spectral response of 12×400 GHz AWG with 70 waveguides used in the array.

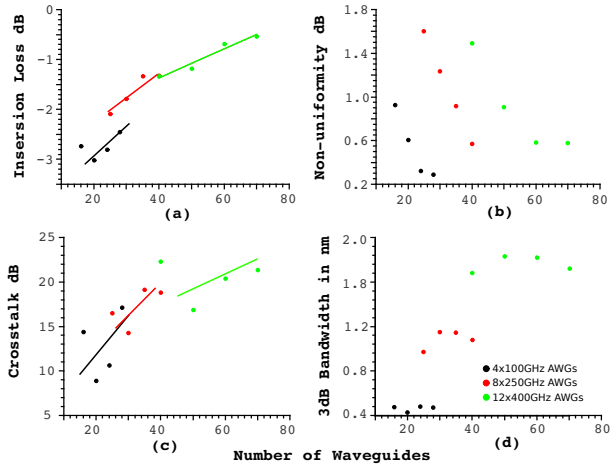

Fig. 6. (a) Insertion loss variation (b) non-uniformity variation (c) cross talk variation and (d) bandwidth variation with the variation of the number of waveguides used in the array waveguides for 4×100 GHz, 8×250 GHz and 12×400 GHz AWGs.

be seen from Fig. 6(c) improves considerably when increasing the channel spacing. This improvement originates both from an improved center channel loss for the larger channel spacing devices and from an improving crosstalk floor. Within one device group (with fixed channel spacing) the crosstalk level increases when increasing the number of waveguides within the array. In this case the crosstalk floor remains nearly constant between devices but the central channel loss improves significantly. It is expected that further increasing the number of waveguides results in array waveguides will not further improve the performance given that in that case the waveguides in the array start to couple, introducing a new crosstalk channel.

4.C. Bandwidth

Within a group of devices we expect the bandwidth to be constant as the channel spacing and the star coupler size were fixed. But from Fig. 6(d) we can see some small variation in the 3dB bandwidth. A possible explanation are random shape changes of a wavelength channel due to variations in the line widths and local wafer thickness. Alternatively it could be due to a ripple in the transfer characteristics caused by parasitic reflections at the fiber couplers introducing uncertainty on the exact shape of the AWG transfer function.

5. Conclusion

We demonstrated compact SOI based arrayed waveguide gratings (AWG) for (de)multiplexing applications with a wide range of wavelength resolutions. The performance of the devices in terms of insertion loss, crosstalk and non-uniformity improves when we use a larger free spectral range (FSR), and this without increasing the footprint of the device. The best performance is achieved for 4×100 GHz, 8×250 GHz and 12×400 GHz AWGs with an FSR of 6.9nm, 24.8nm, 69.8nm respectively. For these AWGs we measured an insertion loss of -2.45dB, -1.32dB and -0.53dB respectively. The crosstalk levels of the AWGs are between 17.12dB to 21.37dB and the non-uniformities vary between 0.286dB to 0.567dB. The footprint of the 100 GHz, 250 GHz and 400 GHz AWGs is 1180×285μm^2, 540×320μm^2 and 380×330μm^2 respectively. These results demonstrate that we are able to design and fabricate large FSR SOI-based AWG (de)multiplexers for a wide range of wavelength resolutions with an acceptable performance.

Acknowledgment

The authors acknowledge the multi-project-wafer (MPW) service ePIXfab through which the devices were fabricated and part of this work was supported by the European Research Council through the ERC Inspectra project.

References

[1] K. Takada, M. Abe, M. Shibata, M. Ishii, and K. Okamoto, IEEE Photon. Tech. Lett. **13,** 11 (2001).
[2] C. Dragone, IEEE Photon. Tech. Lett. **3,** 9 (1991).
[3] R. Adar, C. Henry, C. Dragone, R. Kistler, and M. Milbrodt, J. Lightwave Tech. **11,** 2 (1993).
[4] R. Mestric, H. Bissessur, B. Martin, and A. Pinquier, IEEE Photon. Tech. Lett. **8,** 5 (1996).
[5] W. Bogaerts, S. Selvaraja, P. Dumon, J. Brouckaert, K. De Vos, D. Van Thourhout, and R. Baets, IEEE J. Sel. Top. in Quant. Elec., **16,** 1 (2010).
[6] S. Pathak, M. Vanslembrouck, P. Dumon, D. Van Thourhout, and W. Bogaerts, J. Lightwave Tech., **31,** 1 (2013).
[7] J. Zou, X. Jiang, X. Xia, T. Lang, and J.-J. He, J. Lightwave Tech., **31,** 12 (2013).
[8] A. Klekamp, and R. Munzner, J. Lightwave Tech., **21,** 9 (2003).
[9] S. Selvaraja, P. Jaenen, W. Bogaerts, D. Van Thourhout, P. Dumon, and R. Baets, J. Lightwave Tech., **27,** 18 (2009).
[10] F. van Laere, G. Roelkens, M. Ayre, J. Schrauwen, D. Taillaert, D. Van Thourhout, T. Krauss, and R. Baets, J. Lightwave Tech., **25,** 1 (2007).

References

[1] K. Takada, M. Abe, M. Shibata, M. Ishii, and K. Okamoto, Low crosstalk 10ghz spaced 512 channel arrayed waveguide grating multi/demultiplexer fabricated on a 4 in wafer, IEEE Photonics Technology Letters, vol. 13, no. 11, pp. 1182 1184, nov. 2001.

[2] C. Dragone, An nn optical multiplexer using a planar arrangement of two star couplers, IEEE Photonics Technology Letters, vol. 3, no. 9, pp. 812 815, sept. 1991.

[3] R. Adar, C. Henry, C. Dragone, R. Kistler, and M. Milbrodt, Broad-band array multiplexers made with silica waveguides on silicon, Journal of Lightwave Technology, vol. 11, no. 2, pp. 212 219, feb 1993.

[4] R. Mestric, H. Bissessur, B. Martin, and A. Pinquier, 1.31-1.55 m phased-array demultiplexer on inp, IEEE Photonics Technology Letters, vol. 8, no. 5, pp. 638 640, may 1996.

[5] W. Bogaerts, S. Selvaraja, P. Dumon, J. Brouckaert, K. De Vos, D. Van Thourhout, and R. Baets, Silicon-on-insulator spectral filters fabricated with cmos technology, IEEE Journal of Selected Topics in Quantum Electronics, vol. 16, no. 1, pp. 33 44, jan.-feb. 2010.

[6] S. Pathak, M. Vanslembrouck, P. Dumon, D. Van Thourhout, and W. Bogaerts, Optimized silicon awg with flattened spectral response using an mmi aperture, Journal of Lightwave Technology, vol. 31, no. 1, pp. 8793, 2013.

[7] J. Zou, X. Jiang, X. Xia, T. Lang, and J.-J. He, Ultra-Compact Birefringence-Compensated Arrayed Waveguide Grating Triplexer Based on Silicon-On-Insulator, Journal of Lightwave Technology, vol. 31, no. 12, pp. 19351940, 2013.

[8] A. Klekamp, and R. Munzner, Calculation of imaging errors of AWG, Journal of Lightwave Technology, vol. 21, no. 9, pp. 1978-1986, 2003.

[9] S. Selvaraja, P. Jaenen, W. Bogaerts, D. Van Thourhout, P. Dumon, and R. Baets, Fabrication of photonic wire and crystal circuits in silicon-on-insulator using 193nm optical lithography, Journal of Lightwave Technology, vol. 27, no. 18, pp. 40764083, 2009.

[10] F. van Laere, G. Roelkens, M. Ayre, J. Schrauwen, D. Taillaert, D. Van Thourhout, T. Krauss, and R. Baets, Compact and highly efficient grating couplers between optical fiber and nanophotonic waveguides, Journal of Lightwave Technology, vol. 25, no. 1, pp. 151 156, jan. 2007.